SUMMER QUARTER HYPOXIC WATER CHARACTERISTICS OFF-TAMA RIVER ESTUARY, TOKYO BAY REVEALED BY FIELD AND NUMERICAL SIMULATION ANALYSES

Tanuspong Pokavanich[1], Hiroshi Yagi[2] , Kazuo Nadaoka[3], Hiroshi Ogawa[4], Toshihiro Usui[5], Jota Kanda[6], Kenichiro Shimosako[7] and Shunsuke Kimura[8]

[1]Dept. of Mechanical and Environmental Informatics, Tokyo Institute of Tech., pokavanich.t.aa@m.titech.ac.jp
[2]Aquaculture and Fishing Port Eng. Div., Fisheries Research Agency, yagih@fra.affrc.go.jp
[3]Dept. of Mechanical and Environmental Informatics, Tokyo Institute of Tech., nadaoka@mei.titech.ac.jp
[4]Atmosphere and Ocean Research Institute, The University of Tokyo, Tokyo, Japan, hogawa@ori.u-tokyo.ac.jp
[5] Atmosphere and Ocean Research Institute, The University of Tokyo, Tokyo, Japan, usui@ori.u-tokyo.ac.jp
[6]Tokyo University of Marine Science and Technology, Tokyo, Japan , jkanda@kaiyodai.ac.jp
[7]Dept. of Marine Env. and Eng., Port and Airport Res. Inst., Kanagawa, Japan, shimosako-k83ab@pa.krt.mlit.go
[8]Ministry of Land, Infrastructure, Transport and Tourism, Tokyo, Japan, kimura-s2wk@mlit.go.jp

Highly fluctuating feature of hypoxic water (HW) and anoxic water (AW) were observed during two-months intensive field observation in summer 2006 around Tama River Estuary (TRE), Japan. The HW and AW water at times concentrated along the slope of the mouth of Tama River, appeared close to the water surface, were in the mid-depth and quickly disappeared around the middle of September. Trying to understand this dynamic behavior, we ran high resolution hydrodynamic and water quality simulations. Results suggest that the HW and AW had largely developed around bay-head at the end of June from relatively stable water column and increase of dissolved oxygen consumption in the bottom layer. They were transported back and forth along the bay longitudinal axis by the currents driven by prevailing south and north wind. The termination of the HW and AW water was brought about by the stable north wind in the second half of September that enhance the intrusion of the outer sea well oxygenated water.

Key Words: *Hypoxic water, wind driven current, dissolved oxygen consumption rate, Tokyo Bay*

1. INTRODUCTION

In temperate eutrophicated body of water, water column stratification in summer can aggravate water quality problems. This phenomenon lessens vertical mixing of water column that onset the immoderate growth of phytoplankton in upper layers of water and cut the dissolved oxygen (DO) supplies to the lower layers. These lead to the development of the hypoxic and anoxic water at the lower layers. In Tokyo Bay, over decades, the hypoxic water (HW) and anoxic waters (AW) have appeared in summer and disappeared in winter causing various kinds of coastal environment problems (Fujiwara and Yamada, 2002; Koibuchi and Isobe, 2007; Sohma et al., 2008; Yagi et al., 2008). As part of the environmental impact assessment of a new Haneda Airport runway construction at Tama River Estuary (TRE), the present study aims to clarify the features

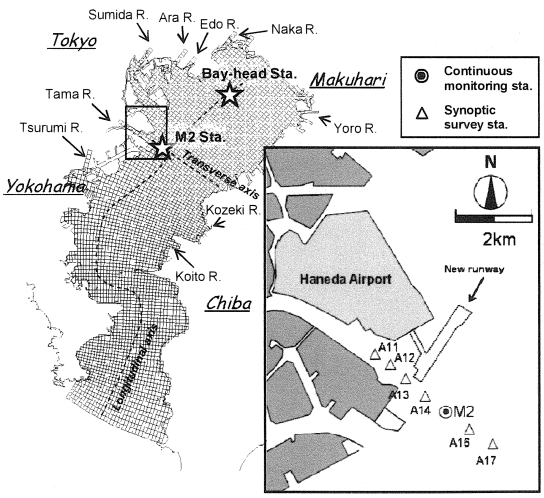

Fig.1 Location of Tokyo Bay and Tama River Estuary, simulation mesh and layout of field observation stations.

of these oxygen-deprived waters as a basis to mitigate the adverse effects of the project to tidal flat ecosystems. We applied intensive field campaigns coupled with high spatial and temporal resolution hydrodynamic and water quality simulations to delineate the development, transport and termination processes of this oxygen-deprived water in summer 2006.

2. FIELD OBSERVATIONS

The intensive field observations were carried out from August to September 2006 along the TRE and at offshore at Sta.M2 (Figure 1). In summary, the hydrographic and water quality data were collected by (1) two-months deployment of data logging sensors using moored buoy, (2) water profiling using AAQ1183 and (3) laboratory analyses of water samples (collected at 12th June; 3rd, 16th, 24th Aug; 1st, 8th, 16th and 22nd September 2006). These data were used to calibrate and validate the bay-scale numerical simulation numerical models.

3. SIMULATION MODELS

The hydrodynamic simulations were carried out using Delft3D-FLOW model in prior to the water quality simulations using Delft3D-WAQ that applied transport conditions from the transport database. The hydrodynamic model includes the following processes: free surface gradients by tidal forcing, wind shear stresses, density differences by water temperature and salinity induced by river discharges and water surface heat fluxes forcing, Coriolis, bed shear stresses, turbulence-induced mass and momentum fluxes and drying and flooding on tidal flats. An irregularly spaced orthogonal horizontal curvilinear grid with sigma coordinate in the vertical was employed. The formulation of the horizontal component of the sub-grid eddy viscosity and sub-grid eddy diffusivity were based on the Horizontal Large Eddy simulation (HLES). Table 1 gives general setup of the model.

Fig. 2 provide the conceptual diagram of the water quality model developed in the present study that includes thirteen state variables (where DetC, DetN, DetP = detritus carbon, nitrogen, phosphorus in the water column; DetCsed, DetNsed, DetPsed = detritus carbon, nitrogen, phosphorus in the sediment, NO3 = nitrate, NH4 = ammonia, PO4 = phosphate) and various interacting processes. The model describes interactions among state variables through physical transport by the current and direct loads through the rivers and bio-chemical processes in terms of oxygen, carbon, nitrogen, phosphorus and inorganic suspended sediment balances. Light attenuation in the water column is a function of suspended phytoplankton, inorganic material, detritus concentration and background value. The general model setup is given in Table 2.

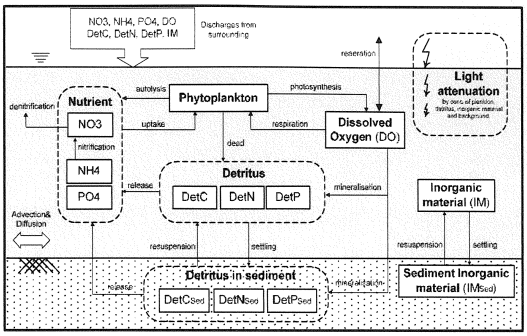

Fig.2 Conceptual diagram of water quality model

Table 1 General setup of hydrodynamic model

Item	Condition
Simulation period	1 June – 1 October 2006 (Spin up in May)
Initial condition	Water temperature: 25 Celsius , Salinity: 34 ppt
Mesh	Horizontal: Orthogonal curvilinear grid 132x44 Verticle: Sima coordinate: 25 layers
Offshore boundary condition	Water level: Observed data at Mera Sta. (JMA). Water temperature & Salinity: Monthly observed profile at Sta.29 (Kanagawa fishery observatory)
River boundary	Discharge: Simulation from other model at Ara R., Sumida R, Tama R., Edo R., Naka R., Tsurumi R., Yoro R., Kozeki R., Koito R. and average sewage discharge Water temperature: Average air temperature Salinity: 0 ppt
Meteorological data	Wind: Observed data at Haneda Airport (JMA) Relative humidity & Air temperature & Could cover: Observed data at Tokyo Station (JMA)
Horizontal eddy estimation	Horizontal Large Eddy Simulation (HLES) model
Vertical eddy estimation	*k-e* model (background eddy viscosity =0.0001 m2/s, background eddy diffusivity =0.000001 m2/s,
Bottom roughness	Chezy 150
Surface heat flux	Procter model. Dalton number. = 0.0015

Table 2 General setup of water quality model

Item	Condition
Simulation period	1 June – 1 October 2006 (Spin up in May)
Initial condition	DO: 3 mgO2/L NO3: 0.20 mgN/L, NH4: 0.15 mgN/L, PO4: 0.10 mgP/L DetC: 1 mgC/L, DetN: 0.2 mgN/L, DetP: 0.03 mgP/L, SS: 2mg/L DetCsed: 10^6 mgC, DetNsed: 10^5 mgN, DetPsed: $0.05*10^5$ mgP, SSsed: 0 mg
Mesh	Horizontal: Orthogonal curvilinear grid 132x44 Verticle: Sima coordinate: 25 layers
Offshore boundary condition	Phytoplankton, PO4, NO3, DO concentration: Representative profile modeled by their relationships with water temperature derived from JODC database NH4: 0.03 mgN/L, DetC: 1 mgC/L, DetN: 0.2 mgN/L , DetP: 0.03 mgP/L, DetC: 2 mg/L
River boundary	Freshwater discharge: Simulation from other model at Ara R., Sumida R, Tama R., Edo R., Naka R., Tsurumi R., Yoro R., Kozeki R. and Koito R. Nutrient concentrations: Estimate from simulated COD, TN, TP from other model with the following assumptions: DetC: 1.46 x COD; NO3: 0.9025 x TN; NH4: 0.0475 x TN; DetN: 0.05 x TN; PO4: 0.53 x TP;DetP: 0.47 x TP
Diffusion	Additional 1 m^2/s to take into consideration the additional movement of water mass that has not yet included in the hydrodynamic model

4. RESULTS AND DISCUSSIONS

(1) Reproducibility of hydrodynamic, water quality and hypoxic water variation

The results of hydrodynamic and water quality model are shown in compare with the observed data in Fig. 3. It is seen that the numerical models can acceptably reproduce the temporal variation of the overall circulation and water quality characteristics at M2 Sta. Generally, surface currents flow in downwind direction. The currents at lower layers flow oppositely to the one of surface and at times independently flow resulting in the two or three strata current structure. The mechanisms behind these complex flow structure are related to the wind and density-driven currents (e.g. Fujiwra and Yamada, 2002; Yagi et al., 2008). Chlorophyll-a concentration (Chl.a conc.) and nutrient concentration dynamic have strong diurnal variation and indicate several phytoplankton blooms (Chl.a conc. > 60 μg/L) those influenced by the dynamic of surface mixed-layer, light availability and transports by and wind-driven circulation (Koibuchi and Isobe, 2007; Pokavanich et al., 2009). In terms of dissolved oxygen concentration (DO conc.), the anoxic condition prevailed in August and first half of September. The concentration abruptly increased near the bottom at 13th September. Fig. 4 illustrates the observed and simulated spatial distribution of DO conc. along the transact of synoptic survey around the TRE suggesting the well reproducibility of the water quality model.

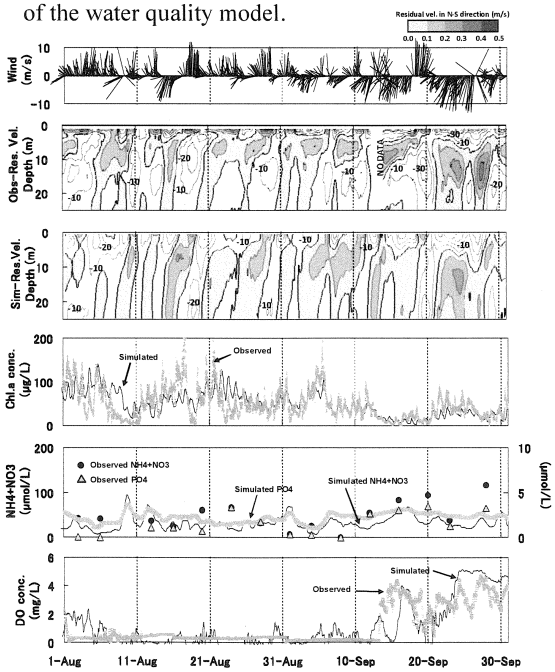

Fig.3 Temporal comparison between observed and simulated hydrographic and water quality parameters at M2 station.

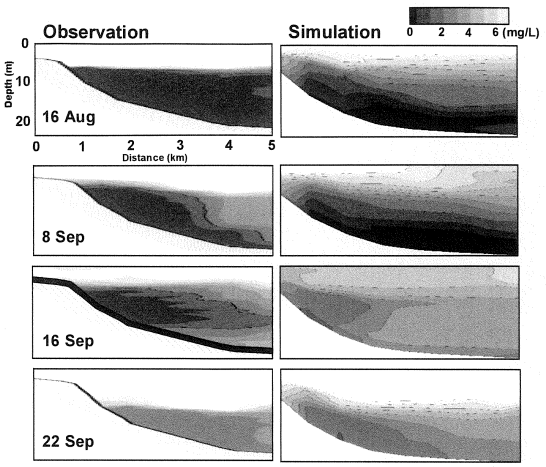

Fig.4 Vertical distribution of dissolved oxygen concentration along the TRE from field and numerical simulation.

(2) Mechanisms of HW generation in Tokyo Bay

The mechanisms of HW generation will be discussed using the temporal variation of the profile of the DO conc., DO consumption rate, water density and water column stability number at bay-head (BH) and M2 station compared with observed wind from the airport given in Fig. 5. The locations of stations are given in Fig. 1. The details of calculation are given in Appendix. The stability number indicates that the surface mixed-layer at the inner part of Tokyo Bay exhibit a dynamic feature and generally extends to the depth of about 10 m. In contrast to the water column at M2 Sta. (which is largely stable below the mixed layer), the water column at BH Sta. has stable periods in June, the end of July and September. The stable water column in June is corresponded to the period of highest water density in the lower layers.

The DO consumption rates have the highest value at the mid-depth at both stations. This feature is affected by the existence of low organic contained seawater in the lower layer as a result of well estuarine circulation of the bay. Therefore, the locally produced detritus has relative short residence time. In addition to the mid-depth high do consumption, at the highest consumption rate can be found at the sea bottom of BH Sta. This indicates that the substantial of the mineralization process of settled-detritus (DetCSed). The DO consumption rate increased at the end of June, especially at BH Sta. This processes together with the lesser supply of DO from the stable water column at the end of June might trigger the development of the HW in summer 2006. The spatial variability of DO consumption rate implies that the HW were largely generated in the bay-head region in consonant with the general higher appearance of HW in this area.

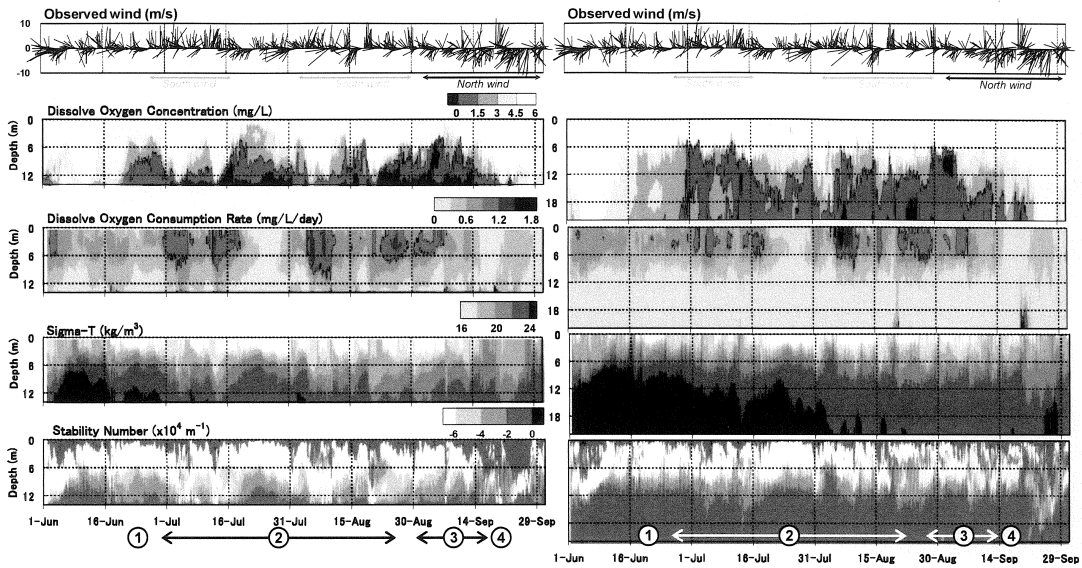

Fig.5 Comparison of the temporal changes the profile of (a) DO concentration, (b) DO consumption rate, (c) density and (d) water column stability number between BH and M2 Sta.

(3) Wind-driven transport and highly fluctuating behavior of HW and AW off the TRE

The prevailing wind play a key role to governed the water circulation in Tokyo Bay has been pointed out extensively in the previous studies (Yagi et al., 2008; Pokavanich et al., 2009). The general wind governing water circulation in this area is described as follows. The south wind results in reversed estuarine circulation where the surface currents flow toward the bay-head and subsurface currents flow toward the bay-mouth. This causes accumulation of coastal water around the bay-head region. In contrast, the north wind enhances the estuarine circulation that the coastal water flow out of the bay in the surface and the sea water flow into the bay underneath. The simulated monthly mean surface and mid-depth velocity field are given in Fig. 6.

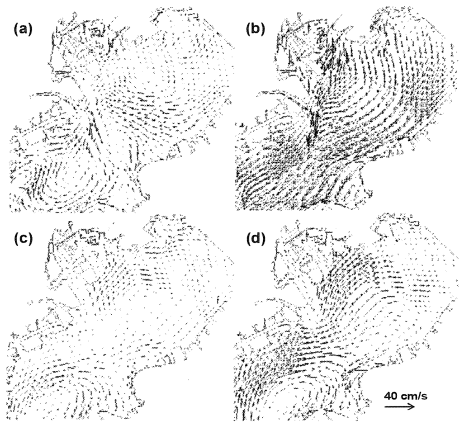

Fig.6 Monthly mean (a), (b) near-surface and (c), (d) mid-depth flow velocity field in August (left column) and September 2006.

Governed by wind-driven circulation, the HW and AW that were generated around the bay head were sloshed back and forth along the bottom and middle-layers of the water column depending on the water column density structure. The mechanisms of hypoxic water transport can be described according the time ① to ④ as indicate in Fig. 5 and summarized in Fig. 6. After the hypoxic water was generated around the bay-head at time ①, at time ② it was spread toward the bay-mouth by the prevailing currents by the south wind. Notice that at the first half of July, the HW appeared in the middle layer at M2 Sta. and after that appeared in the bottom layers. This is a consequence of the strong middle layer outflow resulted from the surface and bottom layer inflow currents driven by the south wind and density different between the inner-bay and outer sea. These HW and AW masses were further spread toward the bay-mouth along the bottom layer by the current governed by prevailing south wind in August. Followed by the relatively stable north in September marked as time ③, these low dissolved oxygen waters were forced to accumulate around the inner-bay by relatively strong inward currents. This feature yielded the upwelling of HW and AW around the bay-head region and the largest appearance of HW.

(4) Mechanisms of HW & AW termination

The termination of hypoxic water period in summer 2006 marks by the abrupt increase of bottom DO conc. around the middle of September

or time ④. In additional to the mechanisms of hypoxic water termination in Tokyo Bay reported by previous studies (e.g. Fujiwara and Yamada, 2002; Yagi et al., 2008), results of the present study strongly indicate a significant role of stable north wind in September. This seasonal prevailing wind enhanced the estuarine circulation that supplies the well oxygenated water from the outer sea and up-welled the oxygen deprived water to the upper layers. The circulation also promoted the gradual seeping in of the oceanic water front along the bay's thalweg. This results in the abrupt increase of DO conc. at M2 Sta. when the front reach at M2 Sta. Fig. 8 provides the spatial distribution of simulated DO conc. compared with the observation before and during the arrival of oceanic water front at M2 Sta.

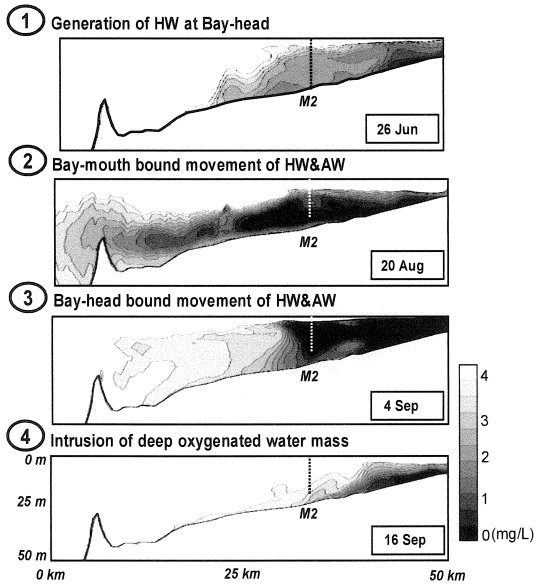

Fig.7 Snapshot of DO conc. along the longitudinal axis at the time corresponds to the key processes discussed in section 4.

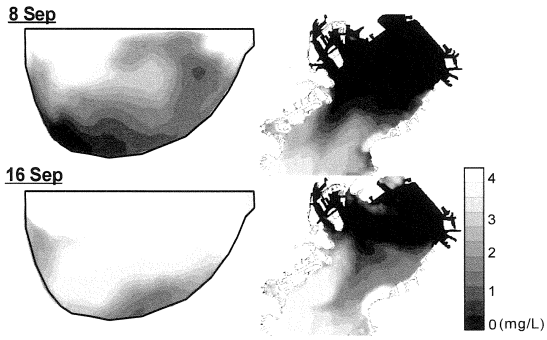

Fig.8 Comparison between dissolved oxygen conc. distribution along bay transverse axis and at the bottom layer before (8 Sep) and during the intrusion of outer sea water (16 Sep).

5. CONCLUDING REMARKS

Results from the present study suggest that the physical, development and fate of HW and AW and other biogeochemical variability of the TRE and inner part of the bay are strongly influenced by the bay-scale processes largely driven by the dynamic of wind and the difference between the inner-bay and the outer sea water properties. These processes can be effectively addressed by the intensive field programs coupled with high resolution numerical simulation models.

ACKNOWLEDGMENT: We thank the Kanagawa Prefectural Fisheries Res. Institute to provide data at Tokyo Bay mouth. This research is supported by Kanto Regional Development Bureau, Ministry of Land, Infrastructure, Transport and Tourism.

APPENDIX:

$$\text{Stability number} = -\frac{1}{\rho}\left(\frac{\partial \rho}{\partial z}\right) \quad (1)$$

$$\text{DO consump.} = \left\{\begin{array}{l}(0.25\times 1.047^{(tem-20)})\times DetC \\ +(0.07\times 1.090^{(tem-20)})\times DetC_{sed}\end{array}\right\}\times 2.67 \quad (2)$$

where ρ is the water density, z is the vertical distance, $DetC$ and $DetC_{sed}$ are the detritus carbon concentration in water column and sediment respectively and tem is the water temperature.

REFERENCES

Sohma, A., Y. Sekiguchi, T., Kuwae, Y. Nakamura (2008): A benthic-pelagic coupled ecosystem model to estimate the hypoxic estuary including tidal-flat-Model description and validation of seasonal/daily dynamics, *Ecological Modelling*, Vol. 215, pp. 10-39.

Fujiwara, T., Y. Yamada (2002): Inflow of oceanic water into Tokyo Bay and generation of a subsurface hypoxic water mass. *Journal of Geophysical Research*, Vol. 107, No. C5, pp. 13.1-10.

Koibuchi, Y., M. Isobe (2007): Phytoplankton bloom mechanism in an area affected by eutrophication: Tokyo Bay in spring 1999. *Coastal Engineering Journal*, Vol. 49, pp. 461-479.

Pokavanich, T., Yagi, H., Nadaoka, K., Ariji, R., Furudo, K., Morohoshi, K., Ogawa H., Usui T., Kanda, J. (2009): Highly fluctuating behavior of hypoxic water off Tama river estuary, Tokyo Bay. Proceeding of 3rd International Conference Estuaries and Coasts, Vol.1, pp. 419-426.

Yagi, H., Pokavanich, T, Yasui, S., Nadaoka, K., Ariji, R., Matsuzaka, S., Suzuki, N., Moroshoshi, Oda, R., Nihei, Y., (2008): Temporal and spatial variations of hypoxic water mass in Tokyo bay governed by the combined effect of coastal upwelling at bay mouth and wind-driven current, *Annual Journal of Coastal Engineering, JSCE*, Vol. 55, No.2, pp. 1081-1085.

(Received June 16, 2010)